$X(5)$ Symmetry to ^{152}Sm

Salah A. Eid[1] and Sohair M. Diab[2]

[1]Faculty of Engineering, Phys. Dept., Ain Shams University, Cairo, Egypt.
[2]Faculty of Education, Phys. Dept., Ain Shams University, Cairo, Egypt.
E-mail: mppe2@yahoo.co.uk

The excited positive and negative parity states, potential energy surfaces, $V(\beta,\gamma)$, electromagnetic transition probabilities, $B(E1)$, $B(E2)$, electric monopole strength $X(E0/E2)$ and staggering effect, $\Delta I = 1$, were calculated successfully using the interacting boson approximation model IBA-1. The calculated values are compared to the available experimental data and show reasonable agreement. The energy ratios and contour plot of the potential energy surfaces show that ^{152}Sm is an $X(5)$ candidate.

1 Introduction

Phase transition is one of the very interesting topic in nuclear structure physics. The even-even samarium series of isotopes have encouraged many authors to study that area extensively experimentally and theoretically.

Experimentally, authors studied levels energy with their half-lives, transition probabilities, decay schemes, multipole mixing ratios, internal conversion coefficients, angular correlations and nuclear orientation of γ-rays[1-4].

Theoretically, different theoretical models have been applied to that chain of isotopes. One of the very interesting models is the interacting boson approximation model IBA [5-10]. Iachello [11,12] has made an important contribution by introducing the new dynamical symmetries $E(5)$ and $X(5)$.

$E(5)$ is the critical point symmetry of phase transition between $U(5)$ and $O(6)$ while $X(5)$ is between $U(5)$ and $SU(3)$ nuclei. The aim of the present work is to calculate:

1. The potential energy surfaces, $V(\beta,\gamma)$;
2. The levels energy, electromagnetic transition rates $B(E1)$ and $B(E2)$;
3. The staggering effect, and
4. The electric monopole strength $X(E0/E2)$.

2 IBA-1 model

2.1 Levels energy

The IBA-1 Hamiltonian [13-16] employed on ^{152}Sm in the present calculation is:

$$\begin{aligned} H &= EPS \cdot n_d + PAIR \cdot (P \cdot P) \\ &+ \frac{1}{2}\, ELL \cdot (L \cdot L) + \frac{1}{2}\, QQ \cdot (Q \cdot Q) \\ &+ 5\, OCT \cdot (T_3 \cdot T_3) + 5HEX \cdot (T_4 \cdot T_4)\,, \end{aligned} \tag{1}$$

where

$$P \cdot p = \frac{1}{2}\left[\begin{array}{l} \left\{(s^\dagger s^\dagger)^{(0)}_0 - \sqrt{5}(d^\dagger d^\dagger)^{(0)}_0\right\} x \\ \left\{(ss)^{(0)}_0 - \sqrt{5}(\tilde{d}\tilde{d})^{(0)}_0\right\} \end{array}\right]^{(0)}_0, \tag{2}$$

$$L \cdot L = -10\,\sqrt{3}\left[(d^\dagger\tilde{d})^{(1)} x\,(d^\dagger\tilde{d})^{(1)}\right]^{(0)}_0\,, \tag{3}$$

$$Q \cdot Q = \sqrt{5}\left[\begin{array}{l} \left\{(S^\dagger\tilde{d} + d^\dagger s)^{(2)} - \frac{\sqrt{7}}{2}\,(d^\dagger\tilde{d})^{(2)}\right\} x \\ \left\{(s^\dagger\tilde{d} + +\tilde{d}s)^{(2)} - \frac{\sqrt{7}}{2}\,(d^\dagger\tilde{d})^{(2)}\right\} \end{array}\right]^{(0)}_0, \tag{4}$$

$$T_3 \cdot T_3 = -\sqrt{7}\left[(d^\dagger\tilde{d})^{(2)} x\,(d^\dagger\tilde{d})^{(2)}\right]^{(0)}_0\,, \tag{5}$$

$$T_4 \cdot T_4 = 3\left[(d^\dagger\tilde{d})^{(4)} x\,(d^\dagger\tilde{d})^{(4)}\right]^{(0)}_0\,. \tag{6}$$

In the previous formulas, n_d is the number of bosons; $P{\cdot}P$, $L{\cdot}L$, $Q{\cdot}Q$, $T_3{\cdot}T_3$ and $T_4{\cdot}T_4$ represent pairing, angular momentum, quadrupole, octupole and hexadecupole interactions respectively between the bosons; EPS is the boson energy; and $PAIR$, ELL, QQ, OCT, HEX are the strengths of the pairing, angular momentum, quadrupole, octupole and hexadecupole interactions respectively (see Table 1).

2.2 Transition rates

The electric quadrupole transition operator employed is:

$$\begin{aligned} T^{(E2)} &= E2SD \cdot (s^\dagger\tilde{d} + d^\dagger s)^{(2)} + \\ &+ \frac{1}{\sqrt{5}}\, E2DD \cdot (d^\dagger\tilde{d})^{(2)}\,. \end{aligned} \tag{7}$$

$E2SD$ and $E2DD$ are adjustable parameters.

The reduced electric quadrupole transition rates between $I_i \to I_f$ states are given by:

$$B(E_2, I_i - I_f) = \frac{[< I_f \parallel T^{(E_2)} \parallel I_i >]^2}{2I_i + 1}\,. \tag{8}$$

3 Results and discussion

In this section we review and discuss the results.

nucleus	EPS	$PAIR$	ELL	QQ	OCT	HEX	$E2SD(eb)$	$E2DD(eb)$
^{152}Sm	0.3840	0.000	0.0084	−0.0244	0.0000	0.0000	0.1450	−0.4289

Table 1: Parameters used in IBA-1 Hamiltonian (all in MeV).

3.1 The potential energy surfaces

The potential energy surfaces [17], $V(\beta, \gamma)$, as a function of the deformation parameters β and γ are calculated using:

$$\begin{aligned} &E_{N_\Pi N_\nu}(\beta,\gamma) = \langle N_\pi N_\nu;\beta\gamma|H_{\pi\nu}|N_\pi N_\nu;\beta\gamma\rangle = \\ &= \zeta_d(N_\nu N_\pi)\beta^2(1+\beta^2) + \beta^2(1+\beta^2)^{-2}\times \\ &\times\left\{kN_\nu N_\pi[4-(\bar{X}_\pi\bar{X}_\nu)\beta\cos 3\gamma]\right\} + \\ &+\left\{[\bar{X}_\pi\bar{X}_\nu\beta^2] + N_\nu(N_\nu-1)\left(\frac{1}{10}c_0+\frac{1}{7}c_2\right)\beta^2\right\}, \end{aligned} \tag{9}$$

where

$$\bar{X}_\rho = \left(\frac{2}{7}\right)^{0.5} X_\rho \, \rho = \pi \text{ or } \upsilon \,. \tag{10}$$

The calculated potential energy surfaces, $V(\beta,\gamma)$, are presented in Figures 1, 2, 3. ^{152}Sm lies between ^{150}Sm which is a vibrational like nucleus, $U(5)$, Fig. 1, while ^{154}Sm is a rotational like, $SU(3)$, nucleus, Fig. 3. So, ^{150}Sm can be an $X(5)$ candidate where levels energy, transition probability ratios as well as the potential energy surfaces are supporting that assumption (see Table 2).

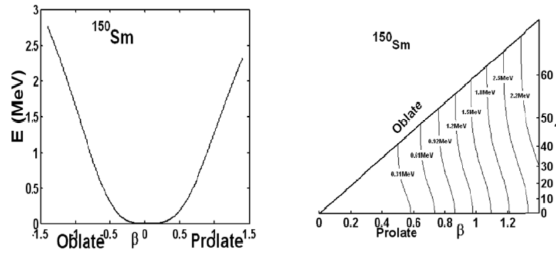

Fig. 1: Potential energy surfaces for ^{150}Sm .

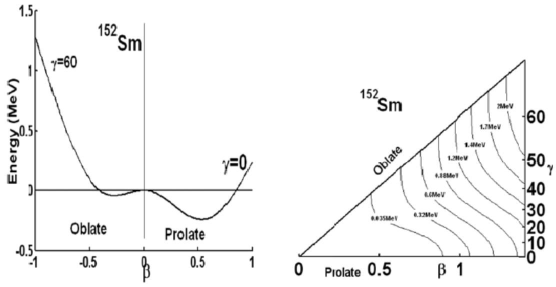

Fig. 2: Potential energy surfaces for ^{152}Sm .

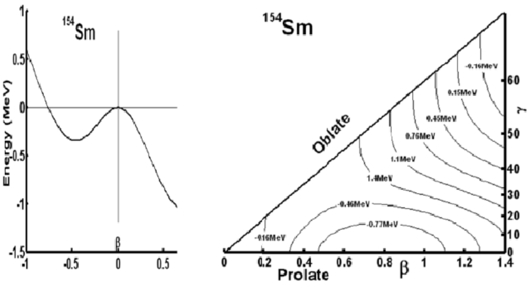

Fig. 3: Potential energy surfaces for ^{154}Sm .

3.2 Energy spectra and electric transition rates

The energy of the positive and negative parity states of ^{152}Sm isotope are calculated using computer code PHINT [19]. A comparison between the experimental spectra [18] and our calculations, using values of the model parameters given in Table 1 for the ground state, $\beta 1$, $\beta 2$ and γ bands are illustrated in Fig. 4. The agreement between the calculated levels energy and their corresponding experimental values are fair, but they are slightly higher especially for the higher excited states in $\beta 1$, $\beta 2$ and γ bands. We believe this is due to the change of the projection of the angular momentum which is due mainly to band crossing. Fig. 5 shows the position of $X(5)$ and $E(5)$ between the other types of nuclei.

Unfortunately there are no available measurements of electromagnetic transition rates $B(E1)$ for ^{152}Sm nucleus, Table 3, while some of $B(E2)$ are measured. The measured $B(E2, 2_1^+ \to 0_1^+)$ is presented, in Table 4, for comparison with the calculated values [20]. The parameters $E2SD$ and $E2DD$ displayed in Table 1 are used in the computer code NPBEM [19] for calculating the electromagnetic transition rates and the calculated values are normalized to $B(E2, 2_1^+ \to 0_1^+)$. No new parameters are introduced for calculating electromagnetic transition rates $B(E1)$ and $B(E2)$ of intraband and interband.

nucleus	$E_{4_1^+}/E_{2_1^+}$	$E_{6_1^+}/E_{2_1^+}$	$E_{8_1^+}/E_{2_1^+}$	$E_{0_2^+}/E_{2_1^+}$	$E_{6_1^+}/E_{0_2^+}$	$E_{0_3^+}/E_{2_1^+}$	$BE2(4_1^+ - 2_1^+)/BE2(2_1^+ - 0_1^+)$
^{152}Sm	3.02	5.83	9.29	5.66	1.03	8.92	1.53
$X(5)$	3.02	5.83	9.29	5.65	1.53	6.03	1.58

Table 2: Energy and transition probability ratios.

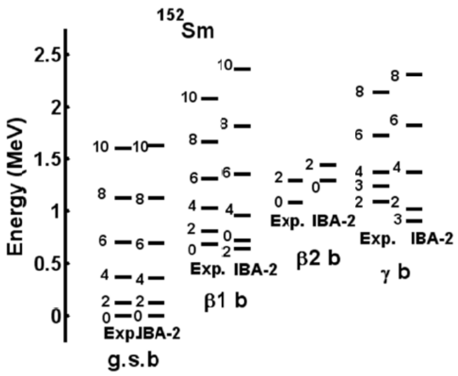

Fig. 4: Experimental[18] and calculated levels energy

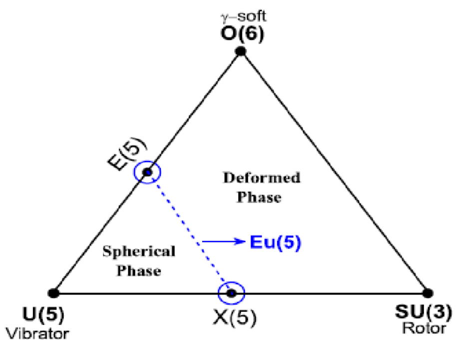

Fig. 5: Triangle showing the position of $X(5)$ and $E(5)$.

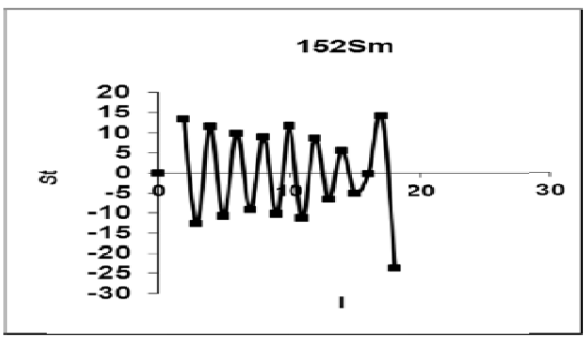

Fig. 6: Staggering effect on ^{152}Sm.

I_i^- I_f^+	$B(E1)$Exp.	$B(E1)$IBA-1
1_1 0_1	—-	0.0979
1_1 0_2	—-	0.0814
3_1 2_1	—-	0.2338
3_1 2_2	—-	0.0766
3_1 2_3	—-	0.0106
3_2 2_1	—-	0.0269
3_2 2_2	—-	0.0291
3_2 2_3	—-	0.0434
5_1 4_1	—-	0.3579
5_1 4_2	—-	0.0672
5_1 4_3	—-	0.0050
7_1 6_1	—-	0.4815
7_1 6_2	—-	0.0574
9_1 8_1	—-	0.6075
9_1 8_2	—-	0.0490
11_1 10_1	—-	0.7367
11_1 10_2	—-	0.0413

Table 3: Calculated $B(E1)$ in ^{152}Sm.

3.3 Staggering effect

The presence of $(+ve)$ and $(-ve)$ parity states has encouraged us to study the staggering effect [21-23] for ^{152}Sm isotope using staggering function equations (11, 12) with the help of the available experimental data [18].

$$St(I) = 6\Delta E(I) - 4\Delta E(I-1) - 4\Delta E(I+1) + \\ + \Delta E(I+2) + \Delta E(I-2)\,, \tag{11}$$

with

$$\Delta E(I) = E(I+1) - E(I)\,. \tag{12}$$

The calculated staggering patterns are illustrated in Fig. 6 and show an interaction between the $(+ve)$ and $(-ve)$ parity states for the ground state band of ^{152}Sm.

3.4 Electric monopole transitions

The electric monopole transitions, $E0$, are normally occurring between two states of the same spin and parity by transferring energy and zero unit of angular momentum. The strength of the electric monopole transition, $X_{if'f}(E0/E2)$, [24] can be calculated using equations (13, 14) and presented in Table 5.

$$X_{if'f}(E0/E2) = \frac{B(E0, I_i - I_f)}{B(E2, I_i - I_{'f})}\,, \tag{13}$$

I_i^+ I_f^+	$B(E2)$Exp*.	$B(E2)$IBA-1
2_1 0_1	0.670(15)	0.6529
3_1 2_1	—-	0.0168
4_1 2_1	0.1.017(4)	1.0014
6_1 4_1	1.179(33)	1.1304
0_2 2_1	0.176(1)	0.3363
2_2 2_1	0.0258(26)	0.0610
2_2 4_1	0.091(11)	0.1057
4_2 2_1	0.0035(35)	0.0003
4_2 4_1	0.037(23)	0.0458
2_3 0_1	0.0163(11)	0.0141
2_3 2_1	0.0417(42)	0.0125
2_3 4_1	0.0416(32)	0.0296
4_3 2_1	0.0035(13)	0.0038
4_3 4_1	0.037(13)	0.0084
4_3 4_2	—-	0.1235
4_3 2_2	—-	0.0070
4_3 2_3	—-	0.3110
4_2 2_2	—-	0.6418
8_1 6_1	—-	1.1681
8_1 6_2	—-	0.0376
10_1 8_1	—-	1.1421

Table 4: Calculated $B(E2)$ in ^{152}Sm (* from Ref.[20])

I_i^+ I_f^+	X(E0/E2)Exp*.	X(E0/E2)IBA-1
0_2 0_1	0.7(0.1)	0.85
0_3 0_2	—-	3.68
0_3 0_1	—-	0.72
0_4 0_3	—-	4.39
0_4 0_2	—-	0.64
0_4 0_1	—-	1.27
2_2 2_1	4.5(0.5)	3.52
2_3 2_1	—-	12.23
2_3 2_2	—-	11.19
4_3 4_1	—-	1.76
4_3 4_2	—-	1.40
4_4 4_1	—-	0.44
4_4 4_2	—-	3.15
4_2 4_1	6.6(2.10)	2.02
6_2 6_1	—-	1.46
8_2 8_1	—-	1.20
10_2 10_1	—-	1.07

Table 5: $X_{if'f}$ $(E0/E2)$ ratios in ^{152}Sm (* from Ref [20]).

where $I_i = I_f = 0$, $I_{'f} = 2$ and $I_i = I_f \neq 0$, $I_f = I_{'f}$.

$$X_{if'f}(E0/E2) = (2.54{\times}10^9)\,A^{3/4} \times \\ \times \frac{E_\gamma^5(\text{MeV})}{\Omega_{KL}}\,\alpha(E2)\,\frac{T_e(E0, I_i - I_f)}{T_e(E_2, I_i - I_{'f})}\,. \tag{14}$$

where:
A : mass number;
I_i : spin of the initial state where E0 and E2 transitions are depopulating it;
I_f : spin of the final state of E0 transition;
$I_{'f}$: spin of the final state of E2 transition;
E_γ : gamma ray energy;
Ω_{KL} : electronic factor for K,L shells [25];
$\alpha(E2)$: conversion coefficient of the E2 transition;
$T_e(E0, I_i - I_f)$: absolute transition probability of the $E0$ transition between I_i and I_f states, and
$T_e(E_2, I_i - I_{'f})$: absolute transition probability of the $E2$ transition between I_i and $I_{'f}$ states.

3.5 Conclusions

The IBA-1 model has been applied successfully to the ^{152}Sm isotope and:

1. Levels energy are successfully reproduced;
2. Potential energy surfaces are calculated and show $X(5)$ characters to ^{152}Sm;
3. Electromagnetic transition rates $B(E1)$ and $B(E2)$ are calculated;
4. Staggering effect has been calculated and beat pattern observed which show an interaction between the $(-ve)$ and $(+ve)$ parity states, and
5. Strength of the electric monopole transitions $X_{if'f}(E0/E2)$ are calculated.

Submitted on January 10, 2016 / Accepted on January 12, 2016

References

1. Qian Y., Ren Z. and Ni D. α-decay half-lives in medium mass nuclei. *J. Phys. G*, 2010, v. 38, 1.
2. Palla G., Geramb H. V. and Pegel C. Electric and inelastic scattering of 25.6 MeV protons from even samarium isotopes. *Nucl. Phys. A*, 1983, v. 403, 134.
3. Talon P., Alamanos N., Lamehi-Rachti M., Levi C. and Papineau L. Coulomb and nuclear excitation effects on ^{16}O scattering from samarium isotopes. *Nucl. Phys. A*, 1981, v. 359, 493.
4. Palla G. and Pegei C. Inelastic scattering of hellions from even-even stable samarium isotopes at 40.9 MeV. *Nucl. Phys. A*, 1979, v. 321, 317.
5. Sabri H. Spectral statistics of rare-earth nuclei: Investigation of shell model configuration effect. *Nucl. Phys. A*, 2015, v. 941, 364.
6. Nomura K., Vretenar D., Nikie T. and Lu B. Microscopic description of octupole shape-phase transitions in light actinide and rare-earth nuclei. *Phys. Rev. C*, 2014, v. 89, 024312.
7. Nikie T., Kralj N., Tutis T., Vretenar D., and Ring P. Implementation of the finite amplitude method for the relativistic quasiparticle random-phase approximation *Phys. Rev. C*, 2013, v. 88, 044327.

8. Nomura K. Interacting boson model with energy density functionals. *J. Phys. Conference Series*, 2013, v. 445, 012015.
9. Nomura K., Shimizu N., and Otsuka T. Formulating the interacting boson model by mean-field methods. *Phys. Rev. C*, 2010, v. 81, 044307.
10. Zhang W., Li Z. P., Zhang S. Q., and Meng J. Octupole degree of freedom for the critical-point candidate nucleus Sm152 in a reflection-asymmetric relativistic mean-field approach. *Phys. Rev. C*, 2010, v. 81, 034302.
11. Iachello F. Dynamic symmetries of the critical point. *Phys. Rev. Lett.*, 2000, v. 85, 3580.
12. Iachello F. Analytic describtion of critical point nuclei in spherical-axially deformed shape phase transition. *Phys. Rev. Lett.*, 2000, v. 85, 3580.
13. Puddu G., Scholten O., Otsuka T. Collective Quadrupole States of Xe, Ba and Ce in the Interacting Boson Model. *Nucl. Phys.*, 1980, v. A348, 109.
14. Arima A. and Iachello F. Interacting boson model of collective states: The vibrational limit. *Ann. Phys.*, 1976, v. 99, 253.
15. Arima A. and Iachello F. Interacting boson model of collective states: The rotational limit. *Ann. Phys.*, 1978, v. 111, 201.
16. Arima A. and Iachello F. Interacting boson model of collective states: The $O(6)$ limit. *Ann. Phys.*, 1979, v. 123, 468.
17. Ginocchio J. N. and Kirson M. W. An intrinisic state for the interacting boson model and its relationship to the Bohr-Mottelson approximation. *Nucl. Phys. A*, 1980, v. 350, 31.
18. Martin M.J. Adopted levels, gammas for ^{152}Sm. *Nucl. Data Sheets*, 2013, v. 114, 1497.
19. Scholten O. The programm package PHINT (1980) version, internal report KVI-63. Keryfysisch Versneller Institut, Gronigen, 1979.
20. Church E. L. and Weneser J. Electron monopole transitions in atomic nuclei. *Phys. Rev.*, 1956, v. 103, 1035.
21. Minkov N., Yotov P., Drenska S. and Scheid W. Parity shift and beat staggering structure of octupole bands in a collective model for quadrupole-octupole deformed nuclei. *J. Phys. G*, 2006, v. 32, 497.
22. Bonatsos D., Daskaloyannis C., Drenska S. B., Karoussos N., Minkov N., Raychev P. P. and Roussev R. P. $\Delta I = 1$ staggering in octupole bands of light actinides Beat patterns. *Phys. Rev. C*, 2000, v. 62, 024301.
23. Minkov N., Drenska S. B., Raychev P. P., Roussev R. P. and Bonatsos D. Beat patterns for the odd-even staggering in octupole bands from quadrupole-octupole Hamiltonian. *Phys. Rev. C*, 2001, v. 63, 044305.
24. Rasmussen J. O. Theory of $E0$ transitions of spheroidal nuclei. *Nucl.Phys.*, 1960, v. 19, 85.
25. Bell A. D., Aveldo C. E., Davidson M. G. and Davidson J. P. Table of $E0$ conversion probability electronic factors. *Can. J. Phys.*, 1970, v. 48, 2542.